Acadlore Transactions on Applied Mathematics and Statistics
https://www.acadlore.com/journals/ATAMS

Analyzing Sensitivity and Solitonic Behavior Using the Dullin-Gottwald -Holm Model in Shallow Water Waves

Shaheera Haroon[1*], Muhammad Abuzar[1], Muhammad Faisal Khan[2]

[1] School of Mathematics, Minhaj University, 54590 Lahore, Pakistan
[2] Department of Science and High Technology, University of Insubria, Via Valleggio 11, 22100 Como, Italy

* Correspondence: Shaheera Haroon (sharoon2409@outlook.com)

Received: 08-25-2023 **Revised:** 09-22-2023 **Accepted:** 09-26-2023

Citation: S. Haroon, M. Abuzar, M. F. Khan, "Analyzing sensitivity and solitonic behavior using the Dullin-Gottwald-Holm model in shallow water waves," *Acadlore Trans. Appl Math. Stat.*, vol. 1, no. 2, pp. 96–110, 2023. https://doi.org/10.56578/atams010205.

Abstract: This paper presents an investigation of traveling wave solutions and a sensitivity analysis for the unidirectional Dullin-Gottwald-Holm (DGH) system, a well-established model for wave propagation in shallow water. We apply the novel auxiliary equation method, a unique integration norm, to extract various soliton solutions, including kink, rational, bright, singular, and bright-singular solutions. Precise explicit solutions of the resultant ordinary differential equations are demonstrated using suitable parametric values. Furthermore, we explore the conditions that ensure the existence of these solutions. By applying the Galilean transformation, we convert the model into a planar dynamical system and evaluate its sensitivity performance. The selection of appropriate parameters enables the generation of two and three-dimensional sketches, as well as contour plots for each solution.

Keywords: Auxiliary equation method; Water wave; Traveling wave results; Sensitivity analysis

1 Introduction

Scientists and engineers are becoming ever more intrigued by the research of nonlinear wave phenomena in a modern global era of science and technology. In many scientific disciplines, nonlinear partial differential equations (NLPDEs) are essential for comprehending nonlinear wave phenomena that constitute our day-to-day challenges. Due to its various uses and applications throughout the past few decades, NLPDEs have therefore attracted a lot of attention in the field of nonlinear sciences. The NLPDEs are crucial in describing the dynamical, physical, and physical processes in many different scientific domains, including ocean engineering, optical fibers, fluid mechanics, plasma physics, quantum physics, geology, biology, and many othersr [1–6]. The behavior of waves in several domains is explained by NLPDEs. In many different branches of science, particularly the study of complex nonlinear wave phenomena, the precise solution of NPDEs is crucial to understanding many physical processes. Since these effective computing packages make it easier to perform complex and laborious algebraic computations, finding the exact solutions has recently grown in importance among scholars [7–11]. The exact solutions of NLPDEs, especially the solitary wave solutions, have a special significance in the soliton theory of mathematical physics. These NLPDE solutions provide more convincing evidence of its physical structures [12–14]. As a result, numerous strong and effective algorithms were developed to derive the exact results for highly nonlinear models. The new auxiliary scheme, out of all of these techniques, is the most effective and reliable for obtaining the precise solution to NLPDEs [15–17].

Analytical exploration and discussion of the DGH system [18] are presented in this research. It has been addressed from a variety of angles, despite not having been analytically addressed yet. The single and combined forms of wave solutions are retrieved under specific parameter conditions, making it pertinent to investigate them analytically. Additionally, the sensitivity analysis is addressed to evaluate how a physical system behaves under stable beginning conditions. The following is how the (1+1)-dimensional DGH-model for shallow water waves is expressed:

$$\mathcal{Q}_t + \theta\mathcal{Q}_x - \varpi^2\left(\mathcal{Q}_{xxt} + \mathcal{Q}\mathcal{Q}_{xxx} + 2\mathcal{Q}_x\mathcal{Q}_{xx}\right) + 3\mathcal{Q}\mathcal{Q}_x + \Lambda\mathcal{Q}_{xxx} = 0, \tag{1}$$

where the velocity of the fluid of the aforementioned system is denoted by $\mathcal{Q}(x,t)$ in the spatial direction x. The coefficients $\varpi^2(\varpi > 0)$ and θ/Λ mention squares of length scales, while $\theta = \sqrt{gh}$ (where $\theta = 2\omega$) denotes the linear wave speed for undisturbed water at rest at spatial infinity. The remarkable repercussions of this DGH system is similar to those of other unidirectional shallow water wave equations.

The DGH equation is a well-known nonlinear evolution equation that is the subject of this article. Many scientists have carefully studied the equation under consideration in order to explain its many aspects. This model has so far been the subject of work. Mustafa [19] has identified the existence and uniqueness of low regularity patterns. Zhou et al. [20] investigated peakon-anti peakon interaction with direct computation. Xiao et al. [21] discussed exact results by employing the traveling-wave transformation and the exp-function technique. The use of qualitative planar systems to describe limited exact traveling wave solutions was examined [22]. Periodic wave solutions were discovered by Meng et al. [23] using integral bifurcation and semi-inverse techniques. To assure a single solution, the ansatz method [24] was also applied. Yu [25] provided examples of the dynamical behavior of traveling wave solutions and related bifurcations in a variety of parameter ranges. da Silva [26] proposed the categorization of bounded traveling wave solutions.

Although this equation has been solved using a variety of analytical and numerical techniques, the new auxiliary equation method (NAEM) has not been performed to examine the governing model before. This approach has also been used to explore different models in multiple studies [27]. On the other hand, this approach makes it much simpler to solve the DGH problem to find novel solutions. Since its beginnings, this approach has gained support from the assessment profession for its straightforward estimation procedure. Future nonlinear scientific discussions will benefit from the findings of this study by having accessibility to excellent research. Future study on this topic may make use of the DGH equation in a fractional sense by applying fractional derivatives because many nowadays researches are focused on solving NLPDEs formulated in the sense of fractional calculus [28–30].

The layout of this article is as follows: Section (2) provides the fundamental idea of the technique. Soliton's solutions have been taken out for the equation in Section (3). Section (4) presents the findings and a discussion of the graphical depiction of the solutions. The sensitive performance of the system is represented in Section (5). Section (6) concludes with final comments.

2 Overview of General Methodology

The solitary wave solutions to the equation under explored are determined by using an analytical scheme that is outlined in this section. A general example of how NLPDE is constructed is the statement that follows:

$$P(\mathcal{Q}, \mathcal{Q}_t, \mathcal{Q}_{tx}, \mathcal{Q}\mathcal{Q}_{tt}, \mathcal{Q}_t\mathcal{Q}_{xx}, ...) = 0, \tag{2}$$

Regarding a specific variable, P is a polynomial function. To transform Eq. (2) into an essential sense of NLODE, take propagational transformation as $\mathcal{Q}(x,t) = U(\zeta)$, where, $\zeta = x - \nu\, t$, then

$$R(U(\zeta), U(\zeta)', U(\zeta)'', U(\zeta)'U(\zeta)'', ...) = 0. \tag{3}$$

The U superscripts signify U's derivative with respect to ζ, thus a polynomial with both linear and nonlinear terms makes up the function R. Using the idea of NAEM, it is now possible to assume the initial solution of Eq. (2) as:

$$U(\zeta) = \sum_{i=0}^{M} \mathfrak{f}_i \lambda^{i\psi(\zeta)}, \tag{4}$$

which satisfy the auxiliary equation

$$\psi'(\zeta) = \frac{1}{ln(\lambda)}\left(\Theta\lambda^{-\psi(\zeta)} + \Phi + \Omega\,\lambda^{\psi(\zeta)}\right), \tag{5}$$

where, $\mathfrak{f}_0$, $\mathfrak{f}_1$, $\mathfrak{f}_2$, ..., $\mathfrak{f}_M$ are unknown coefficients such that $\mathfrak{f} \neq 0$. We can estimate the value of M in accordance with balancing principle by equating the highest nonlinear element in Eq. (3) with the higher level derivative. Here, the various scenarios for possible solutions to Eq. (5) are described.

Case 1: For $\Omega \neq 0$ and $\Phi^2 - 4\Theta\Omega < 0$,

$$\lambda^{\psi(\zeta)} = \frac{-\Phi}{2\Omega} + \frac{\sqrt{4\Theta\Omega - \Phi^2}}{2\Omega}\,\tan\left(\frac{\sqrt{4\Theta\Omega - \Phi^2}}{2}\,\zeta\right), \tag{6}$$

or

$$\lambda^{\psi(\zeta)} = \frac{-\Phi}{2\Omega} - \frac{\sqrt{4\Theta\Omega - \Phi^2}}{2\Omega}\,\cot\left(\frac{\sqrt{4\Theta\Omega - \Phi^2}}{2}\,\zeta\right). \tag{7}$$

Case 2: When $\Phi^2 - 4\Theta\Omega > 0$ and $\Omega \neq 0$,

$$\lambda^{\psi(\zeta)} = \frac{-\Phi}{2\Omega} - \frac{\sqrt{\Phi^2 - 4\Theta\Omega}}{2\Omega} \tanh\left(\frac{\sqrt{\Phi^2 - 4\Theta\Omega}}{2}\,\zeta\right), \tag{8}$$

or

$$\lambda^{\psi(\zeta)} = \frac{-\Phi}{2\Omega} - \frac{\sqrt{\Phi^2 - 4\Theta\Omega}}{2\Omega} \coth\left(\frac{\sqrt{\Phi^2 - 4\Theta\Omega}}{2}\,\zeta\right). \tag{9}$$

Case 3: When $\Phi^2 + 4\Theta^2 < 0$, $\Omega \neq 0$ and $\Omega = -\Theta$,

$$\lambda^{\psi(\zeta)} = \frac{\Phi}{2\Theta} - \frac{\sqrt{-4\Theta^2 - \Phi^2}}{2\Theta} \tan\left(\frac{\sqrt{-4\Theta^2 - \Phi^2}}{2}\,\zeta\right), \tag{10}$$

or

$$\lambda^{\psi(\zeta)} = \frac{\Phi}{2\Theta} + \frac{\sqrt{-4\Theta^2 - \Phi^2}}{2\Theta} \cot\left(\frac{\sqrt{-4\Theta^2 - \Phi^2}}{2}\,\zeta\right). \tag{11}$$

Case 4: When $\Phi^2 + 4\Theta^2 > 0$, $\Omega \neq 0$ and $\Omega = -\Theta$,

$$\lambda^{\psi(\zeta)} = \frac{\Phi}{2\Theta} + \frac{\sqrt{4\Theta^2 + \Phi^2}}{2\Theta} \tanh\left(\frac{\sqrt{4\Theta^2 + \Phi^2}}{2}\,\zeta\right), \tag{12}$$

or

$$\lambda^{\psi(\zeta)} = \frac{\Phi}{2\Theta} + \frac{\sqrt{4\Theta^2 + \Phi^2}}{2\Theta} \coth\left(\frac{\sqrt{4\Theta^2 + \Phi^2}}{2}\,\zeta\right). \tag{13}$$

Case 5: When $\Phi^2 - 4\Theta^2 < 0$ and $\Omega = \Theta$,

$$\lambda^{\psi(\zeta)} = \frac{-\Phi}{2\Theta} + \frac{\sqrt{4\Theta^2 - \Phi^2}}{2\Theta} \tan\left(\frac{\sqrt{4\Theta^2 - \Phi^2}}{2}\,\zeta\right), \tag{14}$$

or

$$\lambda^{\psi(\zeta)} = \frac{-\Phi}{2\Theta} - \frac{\sqrt{4\Theta^2 - \Phi^2}}{2\Theta} \cot\left(\frac{\sqrt{4\Theta^2 - \Phi^2}}{2}\,\zeta\right). \tag{15}$$

Case 6: When $\Phi^2 - 4\Theta^2 > 0$ and $\Omega = \Theta$,

$$\lambda^{\psi(\zeta)} = \frac{-\Phi}{2\Theta} - \frac{\sqrt{-4\Theta^2 + \Phi^2}}{2\Theta} \tanh\left(\frac{\sqrt{-4\Theta^2 + \Phi^2}}{2}\,\zeta\right), \tag{16}$$

or

$$\lambda^{\psi(\zeta)} = \frac{-\Phi}{2\Theta} - \frac{\sqrt{-4\Theta^2 + \Phi^2}}{2\Theta} \coth\left(\frac{\sqrt{-4\Theta^2 + \Phi^2}}{2}\,\zeta\right). \tag{17}$$

Case 7: When $\Phi^2 = 4\Theta\Omega$,

$$\lambda^{\psi(\zeta)} = -\frac{2 + \Phi\,\zeta}{2\Omega\zeta}. \tag{18}$$

Case 8: For $\Theta\Omega < 0$, $\Phi = 0$ and $\Omega \neq 0$,

$$\lambda^{\psi(\zeta)} = -\sqrt{\frac{-\Theta}{\Omega}} \tanh(\sqrt{-\Theta\Omega}\,\zeta), \tag{19}$$

or

$$\lambda^{\psi(\zeta)} = -\sqrt{-\frac{\Theta}{\Omega}} \coth(\sqrt{-\Theta\Omega}\,\zeta). \tag{20}$$

Case 9: When $\Theta = -\Omega$ with $\Phi = 0$,

$$\lambda^{\psi(\zeta)} = -\left(\frac{1 + e^{-2\Omega\,\zeta}}{1 - e^{-2\Omega\,\zeta}}\right). \tag{21}$$

Case 10: For $\Theta = \Omega = 0$,

$$\lambda^{\psi(\zeta)} = \sinh(\Phi\,\zeta) + \cosh(\Phi\,\zeta). \tag{22}$$

Case 11: For $\Theta = \Phi = K$, $\Omega = 0$,

$$\lambda^{\psi(\zeta)} = e^{K\zeta} - 1. \tag{23}$$

Case 12: When $\Omega = \Phi = K$ and $\Theta = 0$,

$$\lambda^{\psi(\zeta)} = \frac{e^{K\zeta}}{1 - e^{K\zeta}}. \tag{24}$$

Case 13: When $\Phi = \Theta + \Omega$,

$$\lambda^{\psi(\zeta)} = -\frac{1 - \Theta e^{(\Theta-\Omega)\zeta}}{1 - \Omega e^{(\Theta-\Omega)\zeta}}. \tag{25}$$

Case 14: When $\Phi = -\Theta - \Omega$,

$$\lambda^{\psi(\zeta)} = \frac{e^{(\Theta-\Omega)\zeta} - \Theta}{e^{(\Theta-\Omega)\zeta} - \Omega}. \tag{26}$$

Case 15: When $\Theta = 0$,

$$\lambda^{\psi(\zeta)} = \frac{\Phi e^{\Phi\zeta}}{1 - \Omega e^{\Phi\zeta}}. \tag{27}$$

Case 16: When $\Theta = \Phi = \Omega \neq 0$,

$$\lambda^{\psi(\zeta)} = \frac{1}{2}\left[\sqrt{3}\ \tan(\frac{\sqrt{3}}{2}\ \Theta\ \zeta) - 1\right]. \tag{28}$$

Case 17: When $\Phi = \Omega = 0$,

$$\lambda^{\psi(\zeta)} = \Theta\ \zeta. \tag{29}$$

Case 18: When $\Phi = \Theta = 0$,

$$\lambda^{\psi(\zeta)} = -\frac{1}{\Omega\ \zeta}. \tag{30}$$

Case 19: For $\Theta = \Omega$ and $\Phi = 0$,

$$\lambda^{\psi(\zeta)} = \tan(\Theta\ \zeta). \tag{31}$$

Case 20: For $\Omega = 0$,

$$\lambda^{\psi(\zeta)} = e^{\Phi\zeta} - \frac{n}{l}. \tag{32}$$

3 Traveling Wave Profile

The objective of this section is to explore into the problem's current traveling wave solutions. We begin with wave transformation to resolve the aforementioned system as $\mathcal{Q}(x,t) = U(\zeta)$ where $\zeta = x - \nu\ t$ such that $\nu \neq 0$. The transformation is substituted into Eq. (1) to produce the following form:

$$\varpi^2\nu U^{'''} - \nu U^{'} + \theta U^{'} - \varpi^2 U U^{'''} + \Lambda U^{'''} + 3UU^{'} - 2\varpi^2 U^{'} U^{''} = 0. \tag{33}$$

Eq. (33) is once integrated with respect to ζ with an integration constant of zero and after some simplification, the above equation becomes

$$U^{''}\big(\varpi^2(-\nu) - \Lambda + \varpi^2 U\big) - \big(\theta - \nu\big)U - \frac{3U^2}{2} + \frac{1}{2}\ \varpi^2 (U^{'})^2. \tag{34}$$

We just apply the homogeneous balance principle to Eq. (34) in order to determine M, resulting in $M = 2$. Now, Eq. (4) has the following shape:

$$U(\zeta) = \mathfrak{f}_0 + \mathfrak{f}_1\lambda^{\psi(\zeta)} + \mathfrak{f}_2\lambda^{2\psi(\zeta)}. \tag{35}$$

By putting Eq. (35) with Eq. (5) into Eq. (34), a system of equations is established by putting all coefficients of different powers of $\lambda^{\psi(\zeta)}$ to zero.

$$
\begin{aligned}
&(\lambda^{\psi(\zeta)})^0 : -2\,\varpi^2\Theta^2\nu\mathfrak{f}_2 + 2\,\varpi^2\Theta^2\mathfrak{f}_0\mathfrak{f}_2 - \Theta\,\Phi\,\Lambda\,\mathfrak{f}_1 - 3/2\,\mathfrak{f}_0{}^2 + \nu\mathfrak{f}_0 - \mathfrak{f}_0 a_0 - 2\,\Theta^2\Lambda\,\mathfrak{f}_2 + \\
&\quad 1/2\,\varpi^2\Theta\nu^2\mathfrak{f}_1{}^2 - \varpi^2\Theta\,\Phi\,\mathfrak{f}_1 + \varpi^2\Theta\,\Phi\,\mathfrak{f}_0\mathfrak{f}_1, \\
&(\lambda^{\psi(\zeta)})^1 : 4\,\varpi^2\Theta^2\mathfrak{f}_1\mathfrak{f}_2 - 6\,\varpi^2\Theta\,\nu\Phi\,\mathfrak{f}_2 - 2\,\varpi^2\Theta\,\nu\Omega\,\mathfrak{f}_1 + 6\,\varpi^2\Theta\,\Phi\,\mathfrak{f}_0\mathfrak{f}_2 + 2\,\varpi^2\Theta\,\Phi\,\mathfrak{f}_1{}^2 + \\
&\quad 2\,\varpi^2\Theta\,\Omega\,\mathfrak{f}_0\mathfrak{f}_1 - \varpi^2\nu\Phi^2\mathfrak{f}_1 + \varpi^2\Phi^2\mathfrak{f}_0\mathfrak{f}_1 - 6\,\Theta\,\Phi\,\Lambda\,\mathfrak{f}_2 - 2\,\Theta\,\Omega\,\Lambda\,\mathfrak{f}_1 - \Phi^2\Lambda\,\mathfrak{f}_1 + \\
&\quad \nu\mathfrak{f}_1 - 3\,\mathfrak{f}_0\mathfrak{f}_1 - \mathfrak{f}_1 a_0, \\
&(\lambda^{\psi(\zeta)})^2 : 4\,\varpi^2\Theta^2\mathfrak{f}_2{}^2 + 3/2\,\varpi^2\Phi^2\mathfrak{f}_1{}^2 - 4\,\Phi^2\Lambda\,\mathfrak{f}_2 - 8\,\varpi^2\Theta\,\nu\Omega\,\mathfrak{f}_2 + 11\,\varpi^2\Theta\,\Phi\,\mathfrak{f}_1\mathfrak{f}_2 + \\
&\quad 8\,\varpi^2\Theta\,\Omega\,\mathfrak{f}_0\mathfrak{f}_2 - 3\,\varpi^2\nu\Phi\,\Omega\,\mathfrak{f}_1 + 3\,\varpi^2\Phi\,\Omega\,\mathfrak{f}_0\mathfrak{f}_1 - 3/2\,\mathfrak{f}_1{}^2 + \nu\mathfrak{f}_2 - \mathfrak{f}_2 a_0 - \\
&\quad 3\,\mathfrak{f}_0\mathfrak{f}_2 + 3\,\varpi^2\Theta\,\Omega\,\mathfrak{f}_1{}^2 - 4\,\varpi^2\nu\Phi^2\mathfrak{f}_2 + 4\,\varpi^2\Phi^2\mathfrak{f}_0\mathfrak{f}_2 - 8\,\Theta\,\Omega\,\Lambda\,\mathfrak{f}_2 - 3\,\Phi\,\Omega\,\Lambda\,\mathfrak{f}_1, \\
&(\lambda^{\psi(\zeta)})^3 : 10\,\varpi^2\Theta\,\Phi\,\mathfrak{f}_2{}^2 + 14\,\varpi^2\Theta\,\Omega\,\mathfrak{f}_1\mathfrak{f}_2 - 10\,\varpi^2\nu\Phi\,\Omega\,\mathfrak{f}_2 - 2\,\varpi^2\nu\Omega^2\mathfrak{f}_1 + 7\,\varpi^2\Phi^2\mathfrak{f}_1\mathfrak{f}_2 + \\
&\quad 10\,\varpi^2\Phi\,\Omega\,\mathfrak{f}_0\mathfrak{f}_2 + 4\,\varpi^2\Phi\,\Omega\,\mathfrak{f}_1{}^2 + 2\,\varpi^2\Omega^2\mathfrak{f}_0\mathfrak{f}_1 - \\
&\quad 10\,\Phi\,\Omega\,\Lambda\,\mathfrak{f}_2 - 2\,\Omega^2\Lambda\,\mathfrak{f}_1 - 3\,\mathfrak{f}_1\mathfrak{f}_2, \\
&(\lambda^{\psi(\zeta)})^4 : 6\,\varpi^2\Phi^2\mathfrak{f}_2{}^2 + 5/2\,\varpi^2\Omega^2\mathfrak{f}_1{}^2 - 6\,\Omega^2\Lambda\,\mathfrak{f}_2 + 17\,\varpi^2\Phi\,\Omega\,\mathfrak{f}_1\mathfrak{f}_2 - 3/2\,\mathfrak{f}_2{}^2 + \\
&\quad 12\,\varpi^2\Theta\,\Omega\,\mathfrak{f}_2{}^2 - 6\,\varpi^2\nu\Omega^2\mathfrak{f}_2 + 6\,\varpi^2\Omega^2\mathfrak{f}_0\mathfrak{f}_2, \\
&(\lambda^{\psi(\zeta)})^5 : 14\,\varpi^2\Phi\,\Omega\,\mathfrak{f}_2{}^2 + 10\,\varpi^2\Omega^2\mathfrak{f}_1\mathfrak{f}_2, \\
&(\lambda^{\psi(\zeta)})^6 : 8\,\varpi^2\Omega^2\mathfrak{f}_2{}^2.
\end{aligned}
$$

By using the Maple software to solve the provided system, the following acceptable solution is produced:

$$\varpi = 0, \quad \mathfrak{f}_0 = -4\Lambda\Omega\Theta, \quad \mathfrak{f}_1 = -4\Lambda\Omega\Phi, \quad \mathfrak{f}_2 = -4\Lambda\Omega^2 \quad \theta = 4\Omega\Lambda\Theta - \Phi^2\Lambda + \nu. \tag{36}$$

The following is the result of inserting Eq. (36) into Eq. (35):

$$U(\zeta) = -4\Lambda\Omega\left[\Theta + \Phi\,\lambda^{\psi(\zeta)} + \Omega\,\lambda^{2\psi(\zeta)}\right]. \tag{37}$$

Eq. (37) yields a variety of surface wave solutions when the solutions identified by Eq. (5) are substituted:
Case 1: When $\Phi^2 - 4\Theta\Omega < 0$ and $\Omega \neq 0$,

$$
\begin{aligned}
U_{1,1}(x,t) = &-4\Lambda\Theta\Omega + 2\Phi\Omega\left[\Phi - \sqrt{4\Theta\Omega - \Phi^2}\tan\left(\frac{\sqrt{4\Theta\Omega - \Phi^2}}{2}\zeta\right)\right] - \\
&\Omega\left[-\Phi + \sqrt{4\Theta\Omega - \Phi^2}\tan\left(\frac{\sqrt{4\Theta\Omega - \Phi^2}}{2}\zeta\right)\right]^2,
\end{aligned} \tag{38}
$$

or

$$
\begin{aligned}
U_{1,2}(x,t) = &-4\Lambda\Theta\Omega + 2\Phi\Omega\left[\Phi + \sqrt{4\Theta\Omega - \Phi^2}\cot\left(\frac{\sqrt{4\Theta\Omega - \Phi^2}}{2}\zeta\right)\right] - \\
&\Omega\left[\Phi + \sqrt{4\Theta\Omega - \Phi^2}\cot\left(\frac{\sqrt{4\Theta\Omega - \Phi^2}}{2}\zeta\right)\right]^2.
\end{aligned} \tag{39}
$$

Case 2: When $\Phi^2 - 4\Theta\Omega > 0$ and $\Omega \neq 0$,

$$
\begin{aligned}
U_{2,1}(x,t) = &-4\Lambda\Theta\Omega + 2\Phi\Omega\left[\Phi + \sqrt{\Phi^2 - 4\Theta\Omega}\tanh\left(\frac{\sqrt{\Phi^2 - 4\Theta\Omega}}{2}\zeta\right)\right] - \\
&\Omega\left[\Phi + \sqrt{\Phi^2 - 4\Theta\Omega}\tanh\left(\frac{\sqrt{\Phi^2 - 4\Theta\Omega}}{2}\zeta\right)\right]^2,
\end{aligned} \tag{40}
$$

or

$$
\begin{aligned}
U_{2,2}(x,t) = &-4\Lambda\Theta\Omega + 2\Phi\Omega\left[\Phi + \sqrt{\Phi^2 - 4\Theta\Omega}\coth\left(\frac{\sqrt{\Phi^2 - 4\Theta\Omega}}{2}\zeta\right)\right] - \\
&\Omega\left[\Phi + \sqrt{\Phi^2 - 4\Theta\Omega}\coth\left(\frac{\sqrt{\Phi^2 - 4\Theta\Omega}}{2}\zeta\right)\right]^2.
\end{aligned} \tag{41}
$$

Case 3: When $\Phi^2 + 4\Theta\Omega < 0$, $\Omega \neq 0$ and $\Omega = -\Theta$,

$$U_{3,1}(x,t) = 4\Theta^2\Omega + 2\Phi\Omega\left[\Phi - \sqrt{-4\Theta^2 - \Phi^2}\tan\left(\frac{\sqrt{-4\Theta^2 - \Phi^2}}{2}\zeta\right)\right] - \Omega\left[\Phi - \sqrt{-4\Theta^2 - \Phi^2}\tan\left(\frac{\sqrt{-4\Theta^2 - \Phi^2}}{2}\zeta\right)\right]^2, \tag{42}$$

or

$$U_{3,2}(x,t) = 4\Theta^2\Omega + 2\Phi\Omega\left[\Phi + \sqrt{-4\Theta^2 - \Phi^2}\cot\left(\frac{\sqrt{-4\Theta^2 - \Phi^2}}{2}\zeta\right)\right] - \Omega\left[\Phi + \sqrt{-4\Theta^2 - \Phi^2}\cot\left(\frac{\sqrt{-4\Theta^2 - \Phi^2}}{2}\zeta\right)\right]^2. \tag{43}$$

Case 4: When $\Phi^2 + 4\Theta\Omega > 0$, $\Omega \neq 0$ and $\Omega = -\Theta$,

$$U_{4,1}(x,t) = 4\Theta^2\Omega + 2\Phi\Omega\left[\Phi + \sqrt{4\Theta^2 + \Phi^2}\tanh\left(\frac{\sqrt{4\Theta^2 + \Phi^2}}{2}\zeta\right)\right] - \Omega\left[\Phi + \sqrt{4\Theta^2 + \Phi^2}\tanh\left(\frac{\sqrt{4\Theta^2 + \Phi^2}}{2}\zeta\right)\right]^2, \tag{44}$$

or

$$U_{4,2}(x,t) = 4\Theta^2\Omega + 2\Phi\Omega\left[\Phi + \sqrt{4\Theta^2 + \Phi^2}\coth\left(\frac{\sqrt{4\Theta^2 + \Phi^2}}{2}\zeta\right)\right] - \Omega\left[\Phi + \sqrt{4\Theta^2 + \Phi^2}\coth\left(\frac{\sqrt{4\Theta^2 + \Phi^2}}{2}\zeta\right)\right]^2. \tag{45}$$

Case 5: When $\Phi^2 - 4\Theta^2 < 0$ and $\Omega = \Theta$,

$$U_{5,1}(x,t) = -4\Theta^2\Omega - 2\Phi\Omega\left[-\Phi + \sqrt{4\Theta^2 - \Phi^2}\tan\left(\frac{\sqrt{4\Theta^2 - \Phi^2}}{2}\zeta\right)\right] - \Omega\left[-\Phi + \sqrt{4\Theta^2 - \Phi^2}\tan\left(\frac{\sqrt{4\Theta^2 - \Phi^2}}{2}\zeta\right)\right]^2, \tag{46}$$

or

$$U_{5,2}(x,t) = -4\Theta^2\Omega + 2\Phi\Omega\left[\Phi + \sqrt{4\Theta^2 - \Phi^2}\cot\left(\frac{\sqrt{4\Theta^2 - \Phi^2}}{2}\zeta\right)\right] - \Omega\left[\Phi + \sqrt{4\Theta^2 - \Phi^2}\cot\left(\frac{\sqrt{4\Theta^2 - \Phi^2}}{2}\zeta\right)\right]^2. \tag{47}$$

Case 6: When $\Phi^2 - 4\Theta^2 > 0$ and $\Omega = \Theta$,

$$U_{6,1}(x,t) = 4\Theta^2\Omega + 2\Phi\Omega\left[\Phi + \sqrt{\Phi^2 - 4\Theta^2}\tanh\left(\frac{\sqrt{\Phi^2 - 4\Theta^2}}{2}\zeta\right)\right] - \Omega\left[\Phi + \sqrt{\Phi^2 - 4\Theta^2}\tanh\left(\frac{\sqrt{\Phi^2 - 4\Theta^2}}{2}\zeta\right)\right]^2, \tag{48}$$

or

$$U_{6,2}(x,t) = 4\Theta^2\Omega + 2\Phi\Omega\left[\Phi + \sqrt{\Phi^2 - 4\Theta^2}\coth\left(\frac{\sqrt{\Phi^2 - 4\Theta^2}}{2}\zeta\right)\right] - \Omega\left[\Phi + \sqrt{\Phi^2 - 4\Theta^2}\coth\left(\frac{\sqrt{\Phi^2 - 4\Theta^2}}{2}\zeta\right)\right]^2. \tag{49}$$

Case 7: When $\Phi^2 = 4\Theta\Omega$,

$$U_7(x,t) = -4\Lambda\Theta\Omega + 4\Lambda\Phi\Omega\left(\frac{2+\Phi\,\zeta}{2\Phi\zeta}\right) - 4\Omega^2\Omega\left(\frac{2+\Phi\,\zeta}{2\Phi\zeta}\right)^2. \tag{50}$$

Case 8: $\Theta\Omega < 0$, $\Phi = 0$ and $\Omega \neq 0$,

$$U_{8,1}(x,t) = -4\Theta\Lambda\Omega - 4\Lambda^2\Omega\left[\sqrt{-\frac{\Theta}{\Omega}}\tanh(\sqrt{-\Theta\Omega}\,\zeta)\right]^2, \tag{51}$$

or

$$U_{8,2}(x,t) = -4\Theta\Lambda\Omega - 4\Lambda^2\Omega\left[\sqrt{-\frac{\Theta}{\Omega}}\coth(\sqrt{-\Theta\Omega}\,\zeta)\right]^2. \tag{52}$$

Case 9: When $\Phi = 0$ and $\Theta = -\Omega$,

$$U_{9,1}(x,t) = 4\Lambda^2\Omega + 4\Lambda^2\Omega\left(\frac{1+e^{-2\,\Omega\,\zeta}}{1-e^{-2\,\Omega\,\zeta}}\right) \tag{53}$$

Case 12: When $\Omega = \Phi = K$ and $\Theta = 0$,

$$U_{12}(x,t) = -4\Lambda\Omega\left[K\left(\frac{e^{K\zeta}}{1-e^{K\zeta}}\right) + K\left(\frac{e^{K\zeta}}{1-e^{K\zeta}}\right)^2\right]. \tag{54}$$

Case 13: When $\Theta + \Omega = \Phi$,

$$U_{13}(x,t) = -4\Lambda\Omega\left[\Theta - \Phi\left(\frac{1-\Theta e^{(\Theta-\Omega)\zeta}}{1-\Omega e^{(\Theta-\Omega)\zeta}}\right) + \Omega\left(\frac{1-\Theta e^{(\Theta-\Omega)\zeta}}{1-\Omega e^{(\Theta-\Omega)\zeta}}\right)^2\right]. \tag{55}$$

Case 14: When $-(\Theta + \Omega) = \Phi$,

$$U_{14}(x,t) = -4\Lambda\Omega\left[\Theta - \Phi\left(\frac{\Theta - e^{(\Theta-\Omega)\zeta}}{e^{(\Theta-\Omega)\zeta}-\Omega}\right) + \Omega\left(\frac{\Theta - e^{(\Theta-\Omega)\zeta}}{e^{(\Theta-\Omega)\zeta}-\Omega}\right)^2\right]. \tag{56}$$

Case 15: When $\Theta = 0$,

$$U_{15}(x,t) = -4\Lambda\Omega\left[\Phi\left(\frac{\Phi\,e^{\Phi\zeta}}{1-\Omega\,e^{\Phi\zeta}}\right) + \Omega\left(\frac{\Phi\,e^{\Phi\zeta}}{1-\Omega\,e^{\Phi\zeta}}\right)^2\right]. \tag{57}$$

Case 16: When $\Phi = \Theta = \Omega \neq 0$,

$$U_{16}(x,t) = -4\Lambda\Omega^2\left[1 + \frac{1}{2}\left(\sqrt{3}\,\tan(\frac{\sqrt{3}}{2}\,\Omega\,\zeta) - 1\right) + \frac{1}{4}\left(\sqrt{3}\,\tan(\frac{\sqrt{3}}{2}\,\Omega\,\zeta) - 1\right)^2\right]. \tag{58}$$

Case 19: When $\Theta = \Omega$ and $\Phi = 0$,

$$U_{19}(x,t) = -4\Lambda\Omega^2\sec^2(\Omega\zeta). \tag{59}$$

4 Results and Discussion

We show a visual representation of these few wave structures that are discovered in the system under study in this section. We employ NAEM to acquire twenty-two precise solutions, and when we compare these solutions, it is clear that the suggested method provides more solutions than the one currently used in the literature for the solution of the DGH equation [19, 26]. By using the proposed technique, wave structures such as kink, rational, hyperbolic, and singular-type wave results are obtained and visually shown via $2D$, $3D$, and their contours plot. These waveforms have various physical significance, as the diagrams demonstrate. For instance, hyperbolic functions like the hyperbolic tangent are used in the computation and speed of special relativity, while the Langevin function for magnetic polarization involves the hyperbolic cotangent [31]. This relationship to the governing model can therefore be explained using the results presented in this work. The findings of this investigation will contribute as motivation and inspiration for the next nonlinear scientific discussions. Our approach is simpler to calculate than previous approaches and is more straightforward, succinct, and effective, and in comparison, to the standard direct methods, it offers more accurate solutions. Figure 1 depicts bright-singular solitons, Figures 2 and 3 showcase bright solitons, Figure 4 illustrates kink solitons, Figure 5 represents singular solitons, Figures 6 and 7 display dark-singular solitons, and Figures 8 and 9 also illustrate kink solitons.

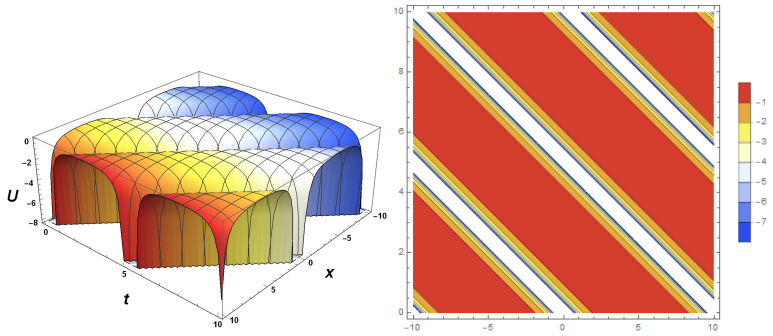

(a) $3D$ (b) Contour plot

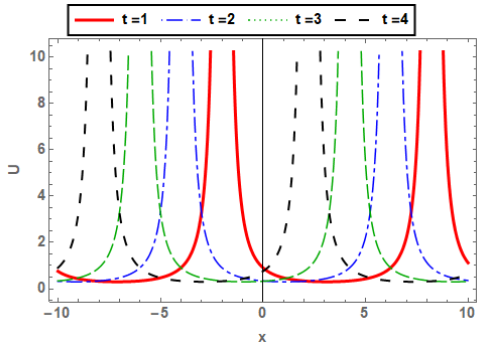

(c) $2D$

Figure 1. Plots (a), (b), and (c) reveal the $3D$, contour, and $2D$ physical behavior of solution $U_{1,2}(x,t)$, respectively, with the parametric values $\Phi = 0.15$, $\Theta = 0.1$, $\Omega = 0.8$, $\Lambda = 1$, and $\nu = -2$

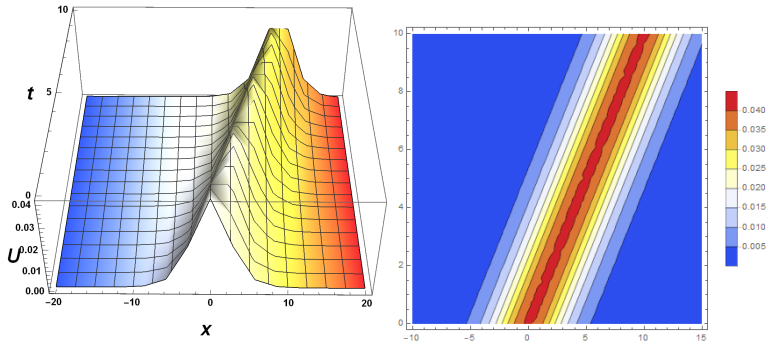

(a) $3D$ (b) Contour plot

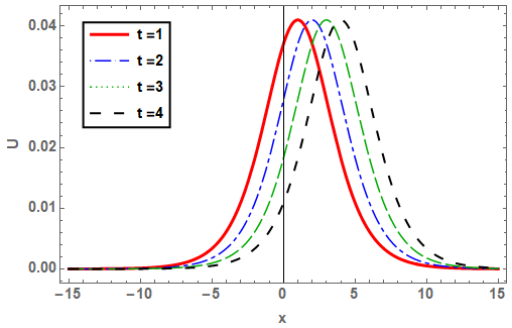

(c) $2D$

Figure 2. Plots of bright soliton wave solution ($U_{2,1}(x,t)$) are represented here by $3D$, contour, and $2D$ respectively, with the parametric values $\Phi = 0.9$, $\Theta = 0.2$, $\Omega = 0.1$, $\Lambda = 0.5$, and $\nu = 1$

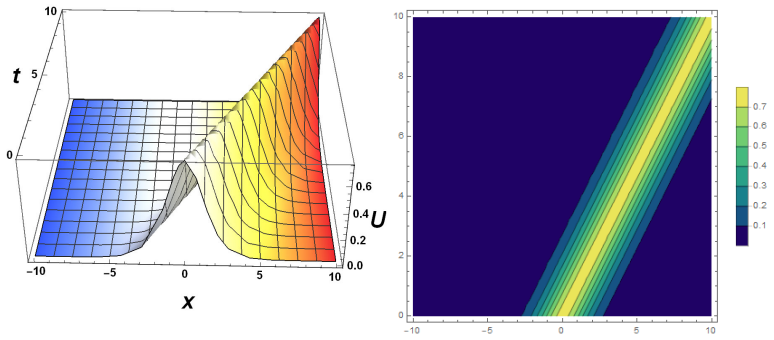

(a) $3D$ (b) Contour plot

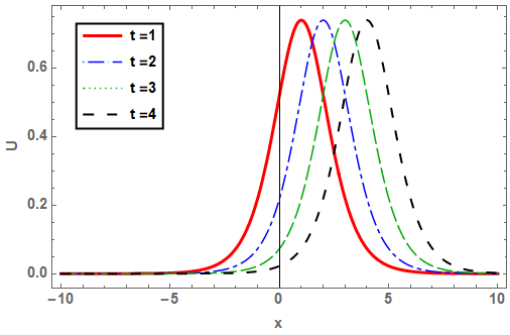

(c) $2D$

Figure 3. Plots (a), (b), and (c) show the $3D$, contour, and $2D$ physical behavior of bright soliton solution $U_{4,1}(x,t)$, respectively, with $\Phi = 1.2$, $\Theta = 0.1$, $\Omega = -0.5$, $\Lambda = -0.1$, and $\nu = 1$

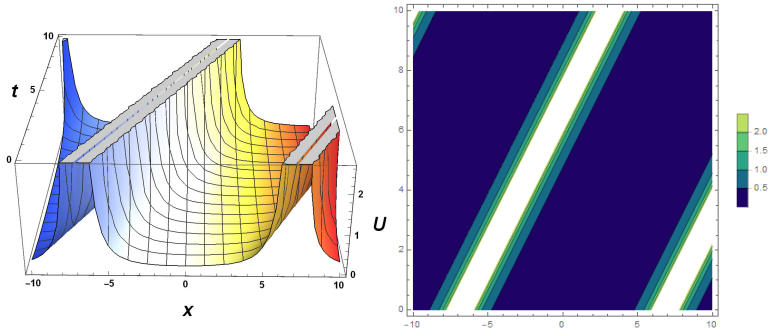

(a) $3D$ (b) Contour plot

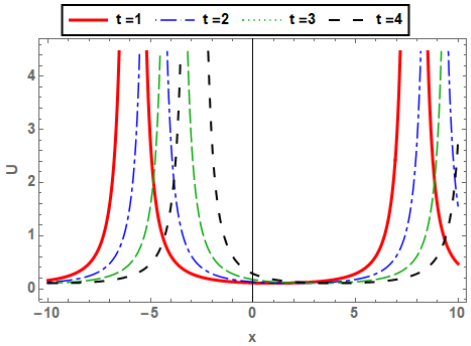

(c) $2D$

Figure 4. Plots (a), (b), and (c) display the $3D$, contour, and $2D$ behavior of combo periodic-singular wave solution $U_{5,1}(x,t)$, respectively, with parametric values $\Phi = 0.2$, $\Theta = \Lambda = 0.25$, $\Omega = -0.5$, and $\nu = 1$

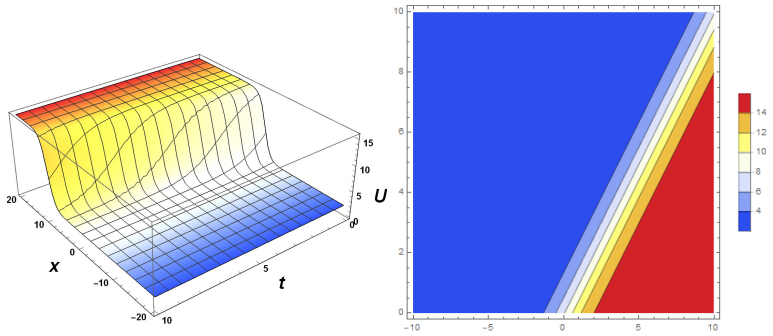

(a) $3D$ (b) Contour plot

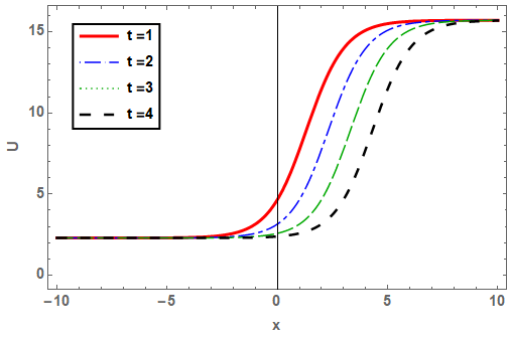

(c) Combine effect of Θ=1 for both operators

Figure 5. Plots (a), (b), and (c) show the $3D$, contour, and $2D$ behavior of kink wave solution $U_{6,1}(x,t)$, respectively, with the parametric values $\Phi = 0.15$, $\Theta = 0.1$, $\Omega = 0.8$, $\Lambda = 1$, and $\nu = -2$

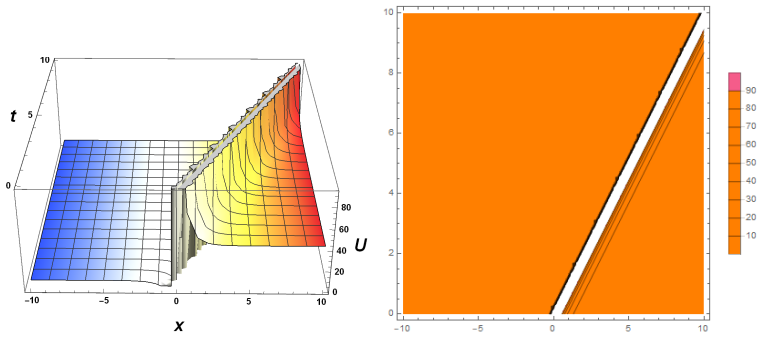

(a) $3D$ (b) Contour plot

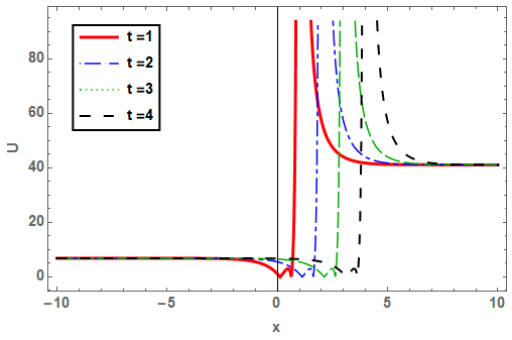

(c) $2D$

Figure 6. Plots (a), (b), and (c) show the $3D$, contour, and $2D$ behavior of singular-type wave solution $U_{6,2}(x,t)$, respectively, with the parametric values $\Phi = 2$, $\Theta = 0.7$, $\Omega = 1.5$, $\Lambda = 0.7$, and $\nu = 1$

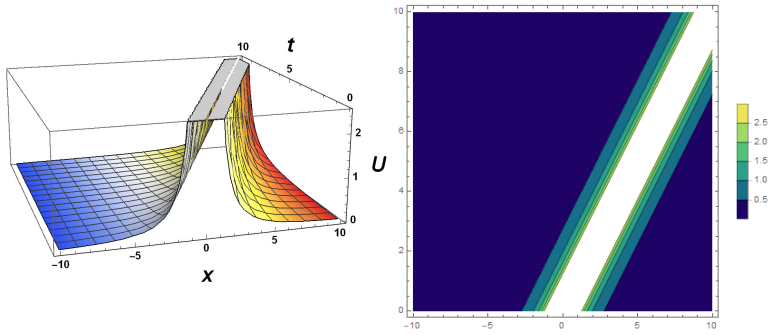

(a) $3D$ (b) Contour plot

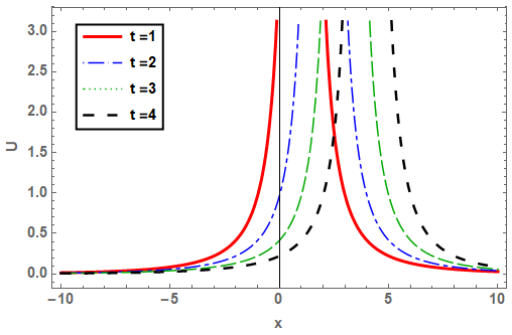

(c) $2D$

Figure 7. Plots (a), (b), and (c) show $3D$, contour, and $2D$ of rational wave solution $U_{12}(x,t)$ are displayed, respectively, with the parametric values $\Phi = 0.3$, $\Theta = 0$, $K = 0.3$, $\Omega = 1$, $\Lambda = 0.3$, and, $\nu = 1$

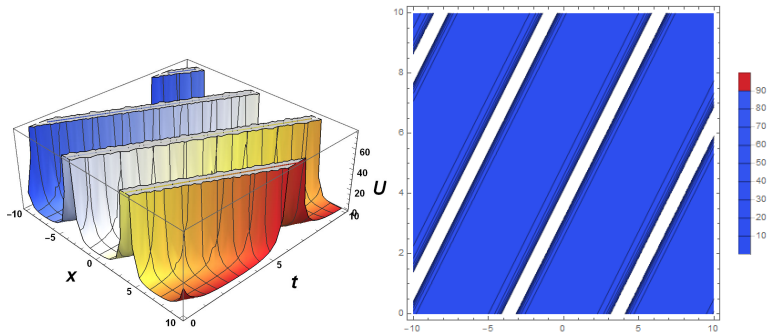

(a) $3D$ (b) Contour plot

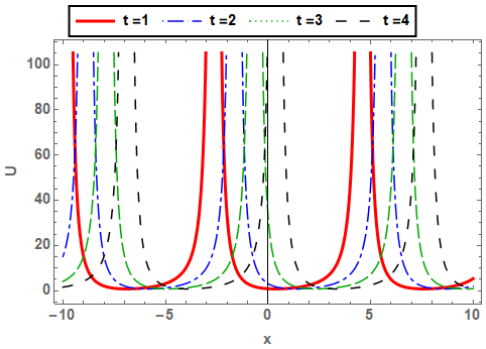

(c) $2D$

Figure 8. Plots (a), (b), and (c) show the $3D$, contour, and $2D$ physical behavior of singular-periodic wave solution $U_{16}(x,t)$, respectively, with the parametric values $\Phi = 1$, $\Theta = 0.5$, $\Omega = 2$, $\Lambda = -0.5$, and $\nu = 1$

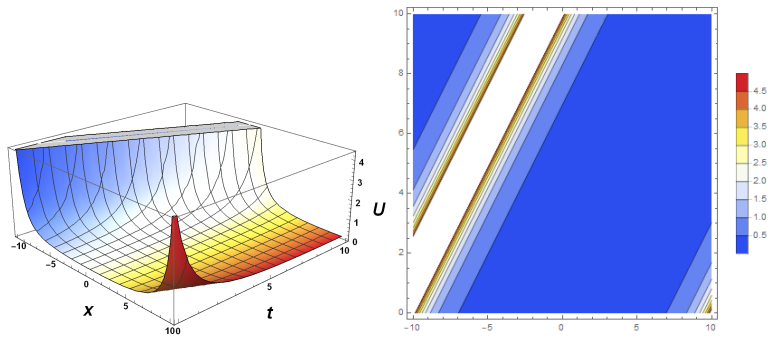

(a) $3D$ (b) Contour plot

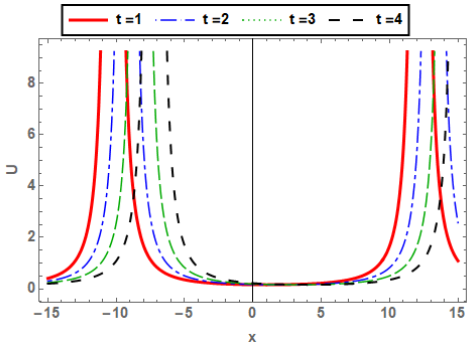

(c) $2D$

Figure 9. Plots (a), (b), and (c) show the $3D$, contour, and $2D$ physical behavior of dark-singular wave solution $U_{19}(x,t)$, respectively, with the parametric values $\Phi = 0$, $\Theta = \Lambda = 0.14$, $\Omega = 2$, and $\nu = 1$

5 Sensitivity Analysis

The sensitive behavior of the suggested model after being transformed into a system is covered in this section. This analysis determines how sensitive our system is to the specified initial and parametric conditions. The system is said to be insensitive if a little change in the beginning conditions only results in a tiny change in the system. Since the system will alter tremendously if the initial conditions vary even slightly, it is highly sensitive. The major objective of this inquiry is to accurately quantify the output disruption caused by changes in input. Here, we'll use the idea of sensitivity analysis to examine Eq. (1). We convert Eq. (31) into the planer dynamical system as a result of studying Galilean transformation:

$$\begin{cases} \frac{dU}{d\zeta} = V, \\ \frac{dV}{d\zeta} = \frac{B}{A}U + \frac{C}{A}U^2 - \frac{D}{A}V^2, \end{cases} \tag{60}$$

where, $A = \left(\varpi^2(U-c) - \Lambda\right)$, $B = \left(\theta - \nu\right)$, $C = \frac{3}{2}$ and $D = \frac{1}{2}\varpi^2$. The above system of equations contains initial conditions namely as: $(0.3, 0.4)$, $(0.3, 0.45)$, $(0.25, 0.45)$, and $(0.3, 0.4)$. The analysis results may be exhibited to show how little changes in the input can cause large variations in the outcome. The results are displayed using a variety of parametric values. Figure 10 reflects the sensitivity of the system taking first initial conditions and Figure 11 shows the behavior of the system when we take a little change in initial conditions and some parameters.

6 Conclusion

The dynamics of novel solitons to the DGH equation has been discussed in this article. In addition to several unique solutions, such as the well-known traveling wave solutions, the achieved solutions include hyperbolic, kink, brilliant, singular, and rational function solutions. NAEM, which is more efficient and has families of solutions, is the technique used to find the solutions. By choosing the appropriate values for the parameter, we also drew some plots to represent the physical behavior of the solutions that were presented. Physically, it can be seen that wave behavior has reported their estimated wave distributions and propagation in Figures 1–9. The calculations also show how useful this method is for locating the exact results from a wider perspective. By selecting various initial conditions and parametric values, the sensitivity analysis to the considered system is also thoroughly examined in Figures 10 and 11. The findings of this study add to the analysis of the DGH equation. The findings of this study

will provide future nonlinear scientific conversations with high-quality literature. One may use DGH equation in a fractional sense applying new fractional derivatives to extend this work in the future [32–35].

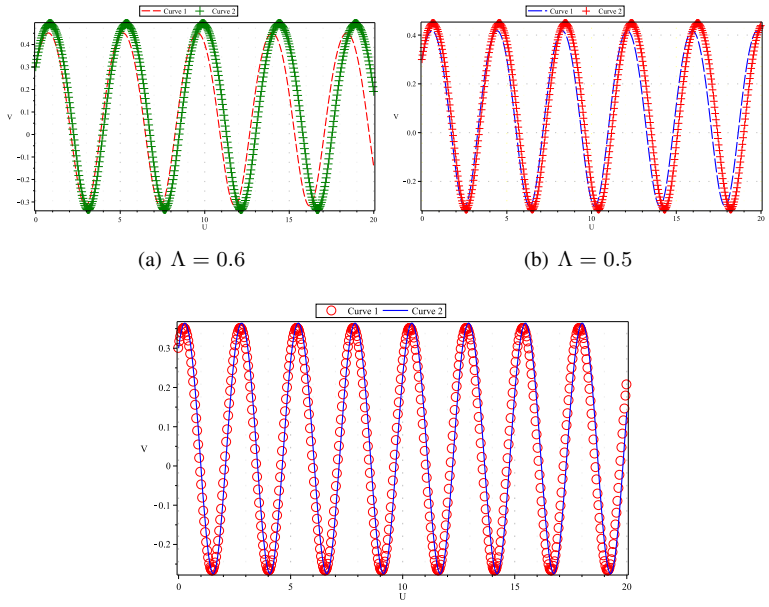

(a) $\Lambda = 0.6$ (b) $\Lambda = 0.5$

(c) $\Lambda = 0.3$

Figure 10. (a), (b) and (c) show the sensitivity analysis of the system by allowing the initial conditions $(0.3, 0.4)$ and $(0.3, 0.45)$ with $\theta = 0.2$, $\nu = 1.4$. $\alpha = 0.3$ with different values of Λ as 0.6, 0.5 and 0.3

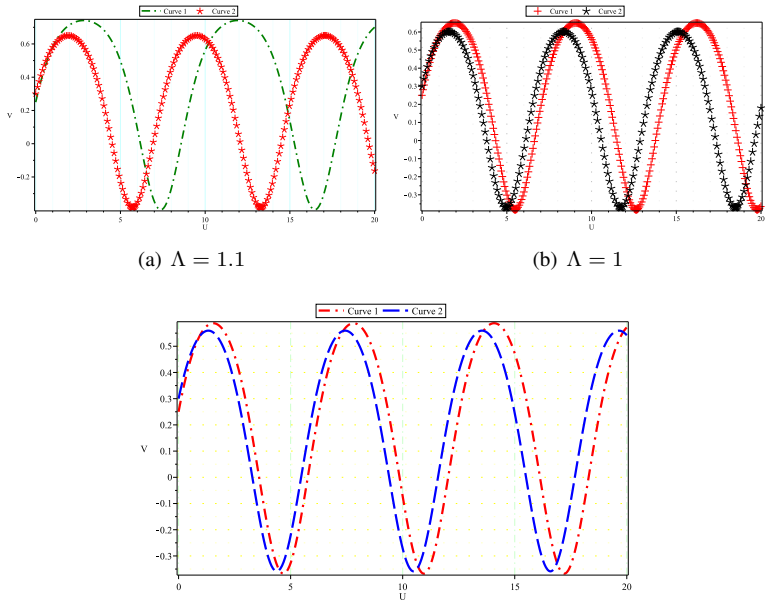

(a) $\Lambda = 1.1$ (b) $\Lambda = 1$

(c) $\Lambda = 0.9$

Figure 11. (a), (b) and (c) represent the sensitivity analysis of the system by allowing the initial conditions $(0.25, 0.45)$, and $(0.3, 0.4)$ with $\alpha = 0.3$, $\nu = 1.4$, $\theta = 0.2$ with three different values of Λ as 1.1, 1 and 0.9

Data Availability

The data used to support the research findings are available from the corresponding author upon request.

Conflicts of Interest

The authors declare no conflict of interest.

References

[1] Y. Shen, B. Tian, C. Cheng, and T. Zhou, "Pfaffian solutions and nonlinear waves of a (3+1)-dimensional generalized Konopelchenko–Dubrovsky–Kaup–Kupershmidt system in fluid mechanics," *Phys. Fluids A*, vol. 35, no. 2, p. 025103, 2023. https://doi.org/10.1063/5.0135174

[2] R. U. Rahman, M. M. M. Qousini, A. Alshehri, M. Sayed Eldin, K. El-Rashidy, and M. Osman, "Evaluation of the performance of fractional evolution equations based on fractional operators and sensitivity assessment," *Results Phys.*, vol. 49, no. 49, p. 106537, 2023. https://doi.org/10.1016/j.rinp.2023.106537

[3] S. E. Savotchenko, "New types of transverse electric nonlinear waves propagating along a linearly graded-index layer in a medium with Kerr nonlinearity," *Opt. Quant. Electron.*, vol. 55, no. 1, p. 74, 2022. https://doi.org/10.1007/s11082-022-04323-1

[4] X. Yao, L. Wang, X. Zhang, and Y. Zhang, "Dynamics of transformed nonlinear waves in the (3+1)-dimensional B-type Kadomtsev–Petviashvili equation II: Interactions and molecular waves," *Nonlinear Dyn.*, vol. 111, no. 5, pp. 4613–4629, 2022. https://doi.org/10.1007/s11071-022-08037-7

[5] R. M. Zulqarnain, W. Ma, M. S. Eldin, K. B. Mehdi, and W. A. Faridi, "New explicit propagating solitary waves formation and sensitive visualization of the dynamical system," *Fractal Fract.*, vol. 7, no. 1, p. 71, 2023. https://doi.org/10.3390/fractalfract7010071

[6] E. AzZobi, A. Alleddawi, I. Alsaraireh, M. Mamat, L. Akinyemi, and H. Rezazadeh, "Novel solitons through optical fibres for perturbed cubic-quintic-septic nonlinear schrodinger-type equation," *Int. J. Nonlinear Anal. Appl.*, vol. 13, no. 1, pp. 1493–506, 2022. https://doi.org/10.22075/ijnaa.2022.5766

[7] Z. Yang, W. Zhong, and M. R. Belić, "Two-dimensional toroidal breather solutions of the self-focusing nonlinear Schrödinger equation," *Phys. Lett. A*, vol. 465, no. A 2023, p. 128715, 2023. https://doi.org/10.1016/j.physleta.2023.128715

[8] H. M. Srivastava, D. Baleanu, J. A. T. Machado, M. S. Osman, H. Rezazadeh, S. Arshed, and H. Günerhan, "Traveling wave solutions to nonlinear directional couplers by modified Kudryashov method," *Phys. Scr.*, vol. 95, no. 7, p. 075217, 2020. https://doi.org/10.1088/1402-4896/ab95af

[9] R. U. Rahman, A. F. Al-Maaitah, M. Qousini, E. A. Az-Zo'bi, M. Sayed Eldin, and M. Abuzar, "New soliton solutions and modulation instability analysis of fractional Huxley equation," *Results Phys.*, vol. 44, no. 44, p. 106163, 2023. https://doi.org/10.1016/j.rinp.2022.106163

[10] J. S. Pickett, S. W. Kahler, L. J. Chen, R. L. Huff, O. Santolík, Y. Khotyaintsev, P. M. E. Décréau, D. Winningham, R. Frahm, M. L. Goldstein, G. S. Lakhina, B. T. Tsurutani, B. Lavraud, D. A. Gurnett, M. André, A. Fazakerley, A. Balogh, and H. Rème, "Solitary waves observed in the auroral zone: The Cluster multi-spacecraft perspective," *Nonlin. Processes Geophys.*, vol. 11, no. 2, pp. 183–196, 2004. https://doi.org/10.5194/npg-11-183-2004

[11] G. Ullah, M. Saleem, M. Khan, M. Khalid, A. Rahman, and S. Nabi, "Ion acoustic solitary waves in magnetized electron–positron–ion plasmas with Tsallis distributed electrons," *Contrib. Plasma Phys.*, vol. 60, no. 10, 2020. https://doi.org/10.1002/ctpp.202000068

[12] T. Han, Z. Li, K. Shi, and G. Wu, "Bifurcation and traveling wave solutions of stochastic Manakov model with multiplicative white noise in birefringent fibers," *Chaos, Solitons Fractals*, vol. 163, no. 163, p. 112548, 2022. https://doi.org/10.1016/j.chaos.2022.112548

[13] T. Han, Z. Li, and X. Zhang, "Bifurcation and new exact traveling wave solutions to time-space coupled fractional nonlinear Schrödinger equation," *Phys. Lett. A*, vol. 395, no. 395, p. 127217, 2021. https://doi.org/10.1016/j.physleta.2021.127217

[14] T. Han and Z. Li, "Classification of all single traveling wave solutions of fractional coupled Boussinesq equations via the complete discrimination system method," *Adv. Math. Phys.*, vol. 2021, no. 2021, pp. 1–6, 2021. https://doi.org/10.1155/2021/3668063

[15] D. Yang, B. Tian, and Y. Shen, "Generalized Darboux transformation and rogue waves for a coupled variable-coefficient nonlinear Schrödinger system in an inhomogeneous optical fiber," *Chin. J. Phys.*, vol. 82, pp. 182–193, 2023. https://doi.org/10.1016/j.cjph.2023.01.003

[16] R. Hirota, *The Direct Method in Soliton Theory*. Cambridge: Cambridge University Press, 2004.

[17] E. Az-Zo'bi, L. Akinyemi, and A. O. Alleddawi, "Construction of optical solitons for conformable generalized model in nonlinear media," *Mod. Phys. Lett. B*, vol. 35, no. 24, p. 2150409, 2021. https://doi.org/10.1142/s0217984921504091

[18] H. R. Dullin, G. A. Gottwald, and D. D. Holm, "An integrable shallow water equation with linear and nonlinear

dispersion," *Phys. Rev. Lett.*, vol. 87, no. 19, pp. 4501–4507, 2001. https://doi.org/10.1103/physrevlett.87.194501

[19] O. G. Mustafa, "Existence and uniqueness of low regularity solutions for the Dullin-Gottwald-Holm equation," *Commun. Math. Phys.*, vol. 265, no. 1, pp. 189–200, 2006. https://doi.org/10.1007/s00220-006-1532-9

[20] J. Zhou, L. Tian, W. Zhang, and S. Kumar, "Peakon–antipeakon interaction in the Dullin–Gottwald–Holm equation," *Phys. Lett. A*, vol. 377, no. 18, pp. 1233–1238, 2013. https://doi.org/10.1016/j.physleta.2013.03.031

[21] G. Xiao, D. Xian, and X. Liu, "Application of Exp-function method to Dullin–Gottwald–Holm equation," *Appl. Math. Comput.*, vol. 210, no. 2, pp. 536–541, 2009. https://doi.org/10.1016/j.amc.2009.01.017

[22] J. Zhong and S. Deng, "Traveling wave solutions of a two-component Dullin–Gottwald–Holm system," *J. Comput. Nonlinear Dyn.*, vol. 12, no. 3, pp. 31 006–1, 2016. https://doi.org/10.1115/1.4035194

[23] Q. Meng, B. He, Y. Long, and Z. Li, "New exact periodic wave solutions for the Dullin–Gottwald–Holm equation," *Appl. Math. Comput.*, no. 218, pp. 4533–4537, 2011. https://doi.org/10.1016/j.amc.2011.10.035

[24] A. Biswas and A. Kara, "1-Soliton solution and conservation laws of the generalizedDullin–Gottwald–Holm equation," *Appl. Math. Comput.*, vol. 217, no. 2, pp. 929–932, 2010. https://doi.org/10.1016/j.amc.2010.05.085

[25] W. Yu, "Exact solutions and bifurcations for the DGH equation," *J. Appl. Anal. Comput.*, no. 6, pp. 968–980, 2016.

[26] P. L. da Silva, "Classification of bounded travelling wave solutions for the Dullin–Gottwald–Holm equation," *J. Math. Anal. Appl.*, vol. 471, no. 1-2, pp. 481–488, 2019. https://doi.org/10.1016/j.jmaa.2018.10.086

[27] X. Zhu, J. Cheng, Z. Chen, and G. Wu, "New solitary-wave solutions of the Van der Waals normal form for granular materials via new auxiliary equation method," *Mathematics*, vol. 10, no. 15, p. 2560, 2022. https://doi.org/10.3390/math10152560

[28] R. N. Premakumari, C. Baishya, and M. K. A. Kaabar, "Dynamics of a fractional plankton–fish model under the influence of toxicity, refuge, and combine-harvesting efforts," *J. Inequal. Appl.*, vol. 2022, no. 1, 2022. https://doi.org/10.1186/s13660-022-02876-z

[29] S. Chakraverty, R. M. Jena, and S. K. Jena, *Computational Fractional Dynamical Systems: Fractional Differential Equations and Applications*. John Wiley and Sons, 2022.

[30] S. J. Achar, C. Baishya, and M. K. A. Kaabar, "Dynamics of the worm transmission in wireless sensor network in the framework of fractional derivatives," *Math. Methods Appl. Sci.*, vol. 45, no. 8, pp. 4278–4294, 2021. https://doi.org/10.1002/mma.8039

[31] M. Bilal, A. R. Seadawy, M. Younis, S. T. R. Rizvi, and H. Zahed, "Dispersive of propagation wave solutions to unidirectional shallow water wave Dullin–Gottwald–Holm system and modulation instability analysis," *Math. Methods Appl. Sci.*, vol. 44, no. 5, pp. 4094–4104, 2020. https://doi.org/10.1002/mma.7013

[32] M. Abu-Shady and M. K. A. Kaabar, "A generalized definition of the fractional derivative with applications," *Math. Prob. Eng.*, vol. 2021, no. 2021, pp. 1–9, 2021. https://doi.org/10.1155/2021/9444803

[33] F. Martínez and M. K. A. Kaabar, "A novel theoretical investigation of the Abu-Shady–Kaabar fractional derivative as a modeling tool for science and engineering," *Comput. Math. Methods Med.*, vol. 2022, pp. 1–8, 2022. https://doi.org/10.1155/2022/4119082

[34] M. J. Ablowitz, J. B. Been, and L. D. Carr, "Fractional integrable nonlinear soliton equations," *Phys. Rev. Lett.*, vol. 128, no. 18, p. 184101, 2022. https://doi.org/10.1103/physrevlett.128.184101

[35] M. Abu-Shady and M. K. A. Kaabar, "A novel computational tool for the fractional-order special functions arising from modeling scientific phenomena via Abu-Shady–Kaabar fractional derivative," *Comput. Math. Methods Med.*, vol. 2022, pp. 1–5, 2022. https://doi.org/10.1155/2022/2138775